*Biochemical Journal* (2021) **478** 1471–1484
https://doi.org/10.1042/BCJ20200664

Research Article

# Syntaxins 6 and 8 facilitate tau into secretory pathways

**Wei Siang Lee[1], Daniel CS Tan[1], Yuanyuan Deng[1], Annika van Hummel[1], Stefania Ippati[1,*], Claire Stevens[1,†], Paulina Carmona-Mora[2,‡], Daryl Ariawan[1], Liming Hou[1], Holly Stefen[1], Tamara Tomanic[1], Mian Bi[1], Florence Tomasetig[2], Adam Martin[1], Thomas Fath[1], Stephen Palmer[2], Yazi D. Ke[1,§] and Lars M. Ittner[1§]**

[1]Dementia Research Centre and Department of Biomedical Sciences, Faculty of Medicine, Health and Human Sciences, Macquarie University, Sydney, NSW 2109, Australia; [2]University of New South Wales, Sydney, NSW 2052, Australia

**Correspondence:** Lars M Ittner (lars.ittner@mq.edu.au)

Tau pathology initiates in defined brain regions and is known to spread along neuronal connections as symptoms progress in Alzheimer's disease (AD) and other tauopathies. This spread requires the release of tau from donor cells, but the underlying molecular mechanisms remained unknown. Here, we established the interactome of the C-terminal tail region of tau and identified syntaxin 8 (STX8) as a mediator of tau release from cells. Similarly, we showed the syntaxin 6 (STX6), part of the same SNARE family as STX8 also facilitated tau release. STX6 was previously genetically linked to progressive supranuclear palsy (PSP), a tauopathy. Finally, we demonstrated that the transmembrane domain of STX6 is required and sufficient to mediate tau secretion. The differential role of STX6 and STX8 in alternative secretory pathways suggests the association of tau with different secretory processes. Taken together, both syntaxins, STX6 and STX8, may contribute to AD and PSP pathogenesis by mediating release of tau from cells and facilitating pathology spreading.

## Introduction

The microtubule-associated protein tau is a multi-domain protein that is involved in the dynamics of the microtubule cytoskeleton, intracellular transport and scaffolding and signaling [1]. Tau is a predominantly neuronal protein, where it is enriched in the axon [2]. Human tau is expressed as six different isoforms due to alternative splicing of exons 2, 3 and 10, resulting in inclusion/exclusion of N-terminal inserts (0N/1N/2N) and an additional microtubule binding repeat (3R/4R) [3]. The tau protein harbors 85 putative phosphorylation sites and in a range of neurodegenerative diseases, including Alzheimer' disease (AD) and progressive supranuclear palsy (PSP), tau becomes abnormally phosphorylated [4]. This hyperphosphorylation interferes with normal tau functions and makes it prone to aggregation that eventually leads to its intracellular deposition and neurofibrillary tangle (NFT) formation [5,6].

The tau protein is organized in four major domains; a N-terminal region followed by the proline-rich projection domain and the microtubule-binding repeats [7]. Finally, there is a C-terminal tail region (CTTR). While the N-terminus and the microtubule-binding repeats vary between isoforms due to alternative splicing, the projections domain and the CTTR are shared between all isoforms. As suggested by the name, the microtubule-binding repeats facilitate the interaction of tau with tubulin [8–11]. Additional interaction partners of tau have been described to interact with the N-terminus [12–14] and the projection domain [15,16] indicating specific functions of these domains. However, the function and interaction partners of tau's CTTR remain unknown.

To establish the interactome of tau's CTTR we performed yeast two-hybrid screening and identified several novel interactors. Specifically, we identified STX8 and STX6 as novel CTTR interactors, important for mediating the release of tau from cells via secretory pathways.

*Present address: San Raffaele Scientific Institute, Experimental Imaging Center, 20132 Milan, Italy
†Present address: School of Chemistry and Molecular Bioscience, University of Wollongong and Illawarra Health and Medical Research Institute, Wollongong, NSW 2522, Australia
‡Present address: MIND Institute/Department of Neurology, University of California, Davis, U.S.A.
§Joint senior authors

Received: 17 September 2020
Revised: 17 March 2021
Accepted: 26 March 2021

Accepted Manuscript online: 26 March 2021
Version of Record published: 16 April 2021

PORTLAND PRESS

*Biochemical Journal* (2021) **478** 1471–1484
https://doi.org/10.1042/BCJ20200664

# Results

## Interactome of the tau C-terminal tail region

To identify interaction partners of tau's CTTR, we performed a yeast two-hybrid screen using a human brain cDNA library with the CTTR sequence (aa369–441) as a bait (Figure 1A,B). A comparative screening approach was undertaken using either non-mutant (wild-type, WT) CTTR or a CTTR variant harboring four phosphorylation-mimicking point mutations, S396D, S404D, S409D and S422D (=PM-CTTR) as baits. Following positive clone selection and sequencing, we identified 46 different interaction candidates with both baits (Supplementary Table S1). Of these, 18 were exclusively identified with the WT CTTR, 21 with the PM-CTTR variant as bait and seven were collectively discovered with both baits (Figure 1C).

Subjecting all 46 interactors to STRING analysis revealed two interconnected clusters of proteins, collectively linking 13 candidates (Figure 1D). No other networks with strong links were identified (Supplementary Figure S1). Consistent with this STRING analysis, functional annotation of these interactors to GO terms highlighted proteins of ubiquitin-proteasome and DNA repair pathways in cluster 1, while proteins associated with chaperone activity and purine metabolism grouped in cluster 2, while SNARE proteins resided outside of both clusters (Figure 1D and Supplementary Table S2).

Next, we used co-immunoprecipitation to validate these interaction candidates. Selected interaction candidates from cluster 1 [WD repeat-containing protein 48 (WDR48), proliferating cell nuclear antigen (PCNA), cullin-1 (CUL1) and COP9 signalosome complex subunit 5 (COPS5)], cluster 2 [endoplasmic reticulum chaperone BiP (HSPA5) and activator of 90 kDa heat shock protein ATPase (AHSA1)] as well as a number of other interactors [(CB1 cannabinoid receptor-interacting protein 1 (CNRIP1), SNARE-associated proteins SNAPIN] and STX8 were equipped with C-terminal myc/HA tag for detection. All candidates were individually co-transfected into HEK 293T cells together with either human non-mutant full-length 2N4R tau or 2N4R PM-tau (or MOCK as control). Of the candidates linked to the ubiquitin-proteasome network, WDR48 co-precipitated more with tau than with PM-tau while PCNA, CUL1 and COPS5 co-precipitated equally to both non-mutant tau and PM-tau (Figure 2A). Selected molecular chaperones, HSPA5 and AHSA1, both have similar interactions with non-mutant tau and PM-tau (Figure 2B). This is in line with a previously reported HSPA5-tau interaction [17]. Of the additionally selected candidates, SNAPIN co-precipitated more with non-mutant tau than with PM-tau, while CNRIP1 and STX8 co-precipitated more with PM-tau than non-mutant tau (Figure 2C). Taken together, we established a novel interactome of tau's CTTR including a network of interactors that link this domain of tau to ubiquitin-proteasome, DNA repair, molecular chaperone and purine metabolism networks. Unconnected interactions candidates suggest that the CTTR is linked to a range of other cellular processes.

## STX8 facilitates release of tau from cells

STX8 has been linked to endosomal protein trafficking [18,19]. This raised the question whether STX8 may be involved in trafficking and the possible secretion of tau, a known concept contributing to disease progression in neurodegenerative disease with tau pathology [20–23]. To address this, we transfected non-mutant tau or PM-tau either with a control vector or STX8 in 293T cells, followed by detection of tau (or PM-tau) in the cell culture medium 72 h later. Neither tau nor PM-tau was released from cells co-transfected with a control vector (Figure 3A). In contrast, marked amounts of tau and PM-tau were present in the medium when co-transfected with STX8. Tau and PM-tau expression in the presence and absence of STX8 had no differential impact on cell viability, as determined by standard LDH-based cell viability assay (Figure 3B). To determine whether facilitating tau release from cells is unique to STX8 or is mediated by other interactor(s) of tau's CTTR, the same release assays for SNAPIN, AHSA1, CUL1, HSPA5, PCNA and WDR48 were performed. Neither co-transfection with non-mutant tau nor with PM-tau resulted in a detectable release of non-mutant tau or PM-tau into the culture medium (Figure 3C–H). Taken together, STX8 mediates the release of tau from co-transfected cells. This was a unique feature amongst the new tau CTTR interactors identified in our study.

## Related syntaxin family member STX6 also drives release of tau from cells

STX8 belongs to the large family of syntaxins that includes the phylogenetically closely related STX6 (Figure 4A). Interestingly, STX6 has been linked genetically to the tau-only neurodegenerative condition PSP [24,25]. Therefore, we tested whether STX6, similar to STX8, interacts with tau and facilitates its secretion of tau from cells. Accordingly, we co-transfected 293T cells with STX6 and non-mutant tau or PM-tau. Immunoprecipitation of non-mutant tau or PM-tau co-precipitated similar levels of STX6 from cell extracts,

*Biochemical Journal* (2021) **478** 1471–1484
https://doi.org/10.1042/BCJ20200664

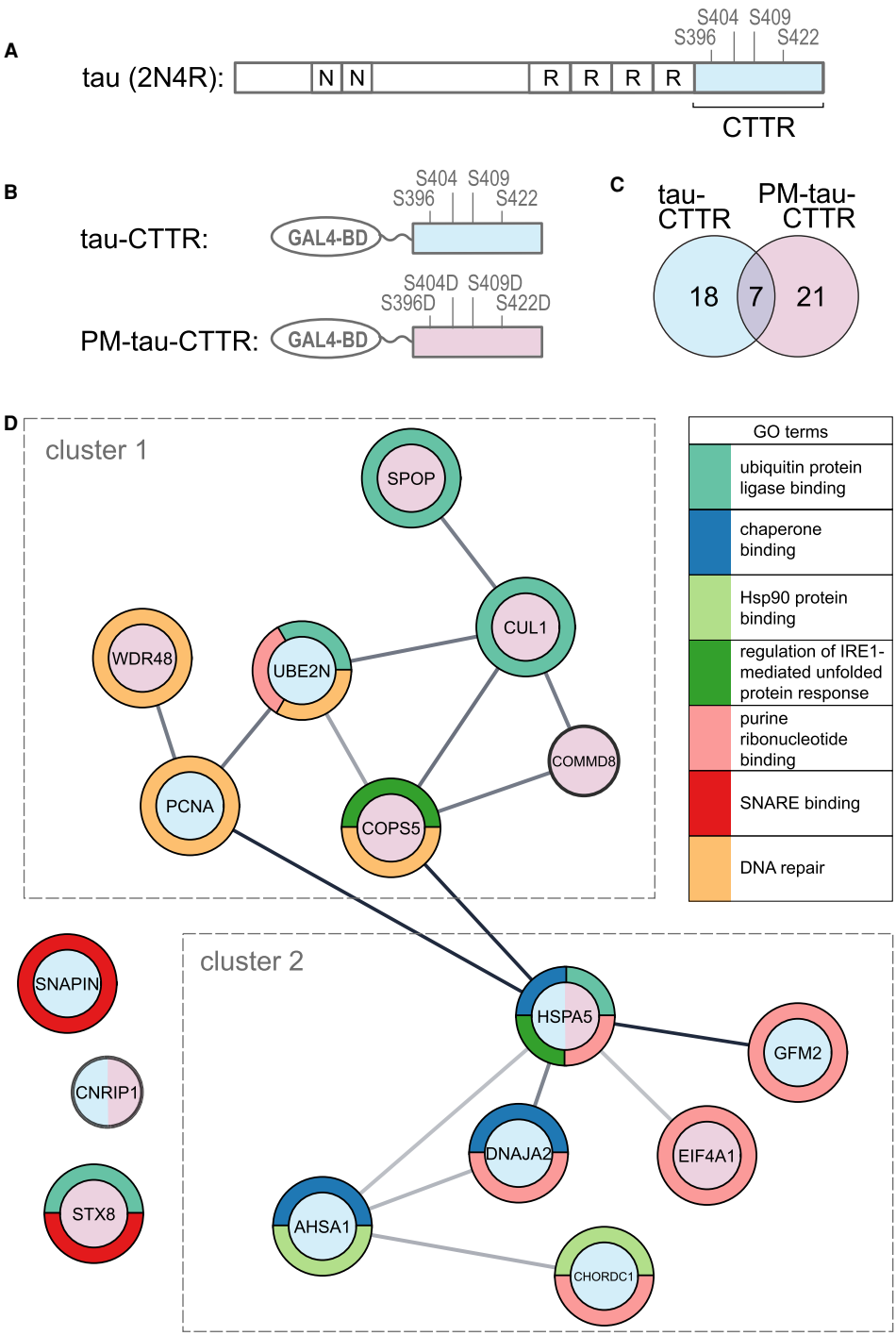


**Figure 1. The tau CTTR interactome.**

(**A**) Schematic of domain structure of human tau isoform 2N4R, including its C-terminal tail region (CTTR, blue). Amino acid positions of phosphorylation sites mutated from Serine (S) to Aspartic Acid (D) in phosphorylation-mimicking variants (PM). N, N-terminal inserts; R, microtubule-binding repeats. (**B**) Illustration of non-mutant human tau-CTTR (blue) or PM-tau-CTTR (pink) baits with the GAL4 DNA binding domain (GAL4-BD) used for yeast-two-hybrid screen (Y2H) of a human CNS cDNA library. (**C**) Venn diagram of candidate interactors by Y2H with the baits CTTR [18], PM-CTTR [21] or both [7]. See Supplementary Table S1 for candidate list. (**D**) STRING clusters (broken boxes) of CTTR (blue) and PM-CTTR (pink) or shared interaction candidates and their GO term annotation (color-coded rings). Additional interactors, SNAPIN, CNRIP1 and STX8, outside the main clusters are displayed. See Supplementary Figure S1 for full STRING network.

*Biochemical Journal* (2021) **478** 1471–1484
https://doi.org/10.1042/BCJ20200664

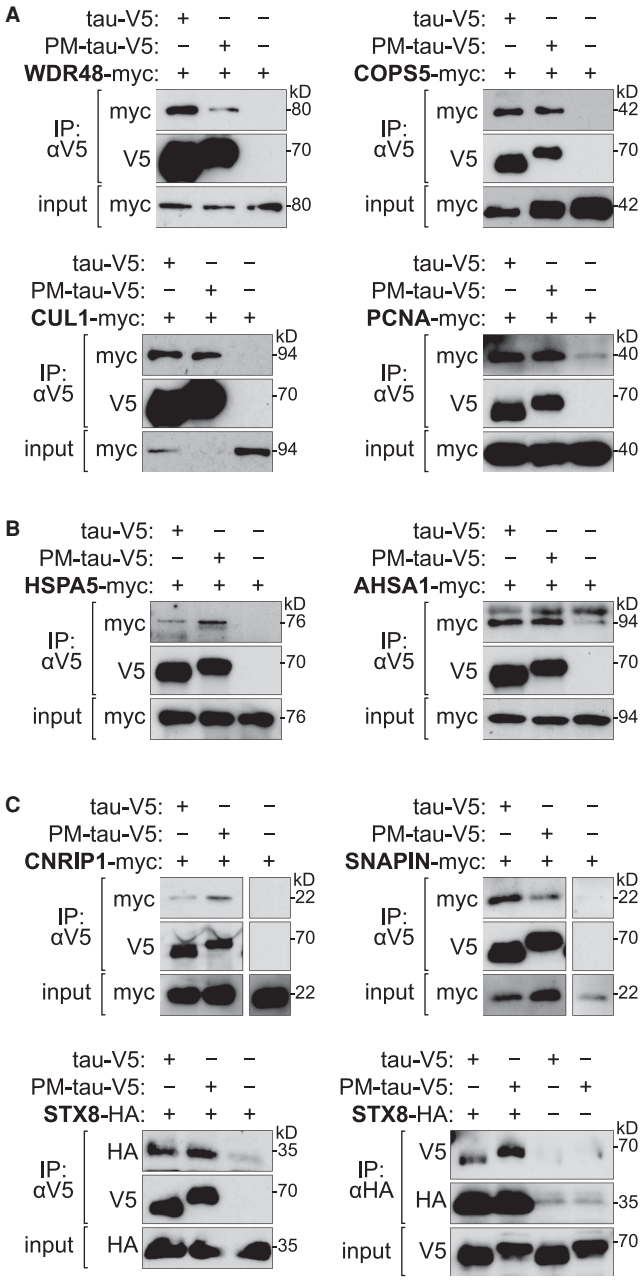


**Figure 2. Tau CTTR interactors.**

(**A**–**C**) Validation of interaction candidates by co-immunoprecipitation (IP) with V5 (αV5) or HA (αHA) antibodies from cells co-expressing myc or HA-tagged candidates and V5-tagged full-length tau or PM-tau. Inputs demonstrate equal expression levels of candidate proteins. Candidates were chosen from (**A**) cluster 1, (**B**) cluster 2 or (**C**) outside these networks (see Supplementary Figure S1).

consistent with an STX6/tau interaction (Figure 4B,C). Immunoprecipitation from the culture medium of co-transfected cells revealed the release of non-mutant tau and PM-tau from cells in the presence of STX6 (Figure 4D). The tau release was not due to cell death since cell viability was comparable between cells transfected with non-mutant tau or PM-tau and those co-transfected with STX6 and tau or PM-tau (Figure 4E). We also addressed whether the individual phosphorylation sites modified in PM-tau contributed differentially to the release facilitated by STX6. Individual phosphorylation-mimicking variants S396D, S404D, S396D/S404S

*Biochemical Journal* (2021) **478** 1471–1484
https://doi.org/10.1042/BCJ20200664

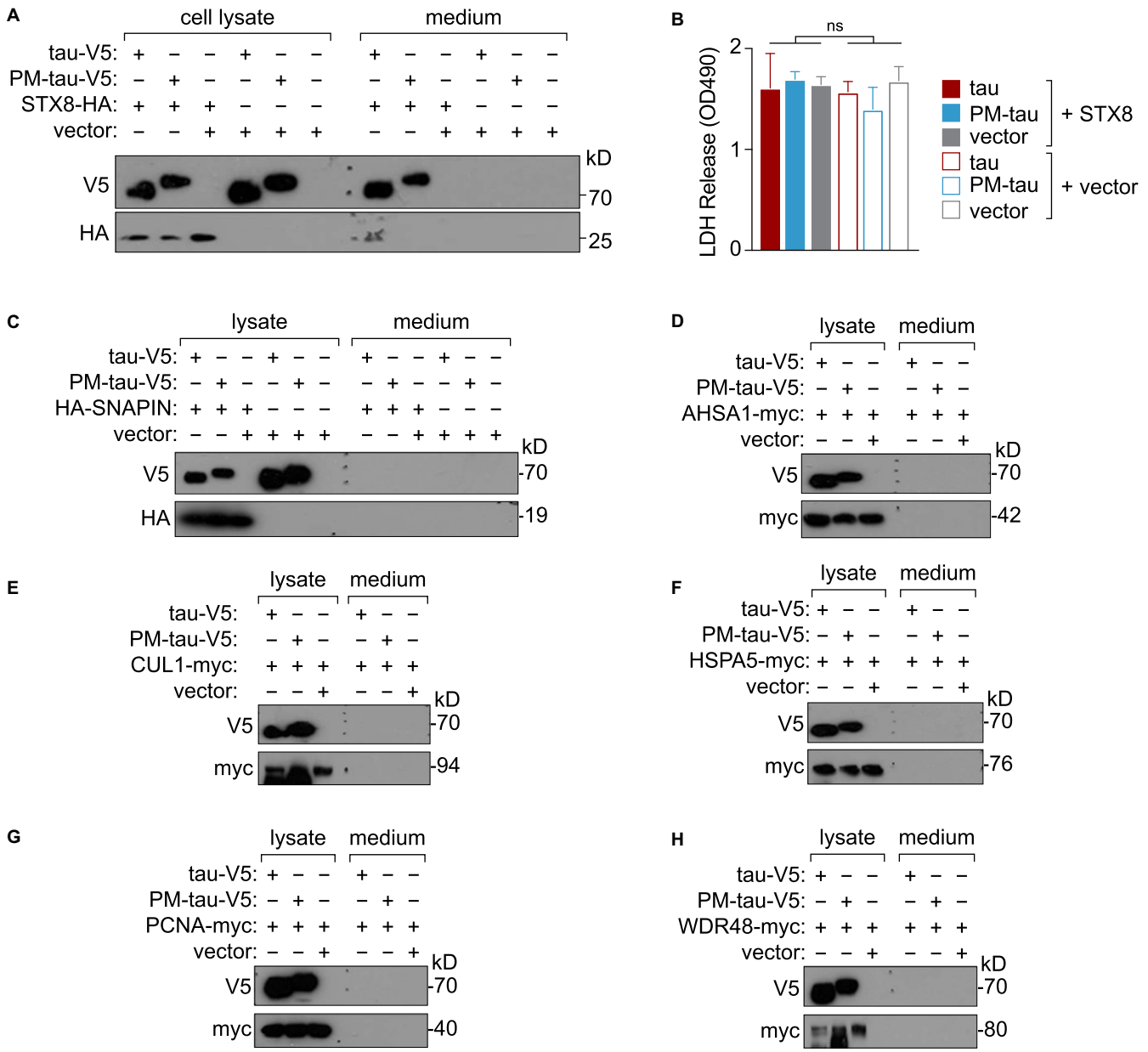


**Figure 3. STX8 mediates tau secretion.**

(**A**) Tau release assay: V5-tagged non-mutant tau and PM-tau (S396D/S404D/S409D/S422D) were released into the medium only when cells were co-transfected with HA-tagged STX8, but not from cells transfected with non-mutant tau and PM-tau together with a vector control. (**B**) Indistinguishable cell viability upon expression of non-mutant tau or PM-tau together with STX8 or a vector control ($n = 3$; ns, not significant; Student's *t*-test). (**C**–**H**) V5-tagged tau and PM-tau (S396D/S404D/S409D/S422D) was absent from culture medium when cells were co-transfected with HA/myc-tagged (C) SNAPIN, (**D**) AHSA1, (**E**) CLU1, (**F**) HSPA5, (**G**) PCNA or (**H**) WDR48. Lysates confirmed expression in transfected cells.

and S422S showed similar levels of release from co-transfected cells in the presence of STX6 (Figure 4D). Levels of release were similar for all phosphorylation-mimicking variants as compared with non-mutant tau. Taken together, we show that STX6 facilitated the release of tau from cells.

## STX6 transmembrane domain is critical for tau secretion

Next, we determined which intrinsic features of STX6 are required for facilitating the secretion of tau. Therefore, we generated a series of different truncation variants of STX6 (Figure 5A). Specifically, we used site-

*Biochemical Journal* (2021) **478** 1471–1484
https://doi.org/10.1042/BCJ20200664

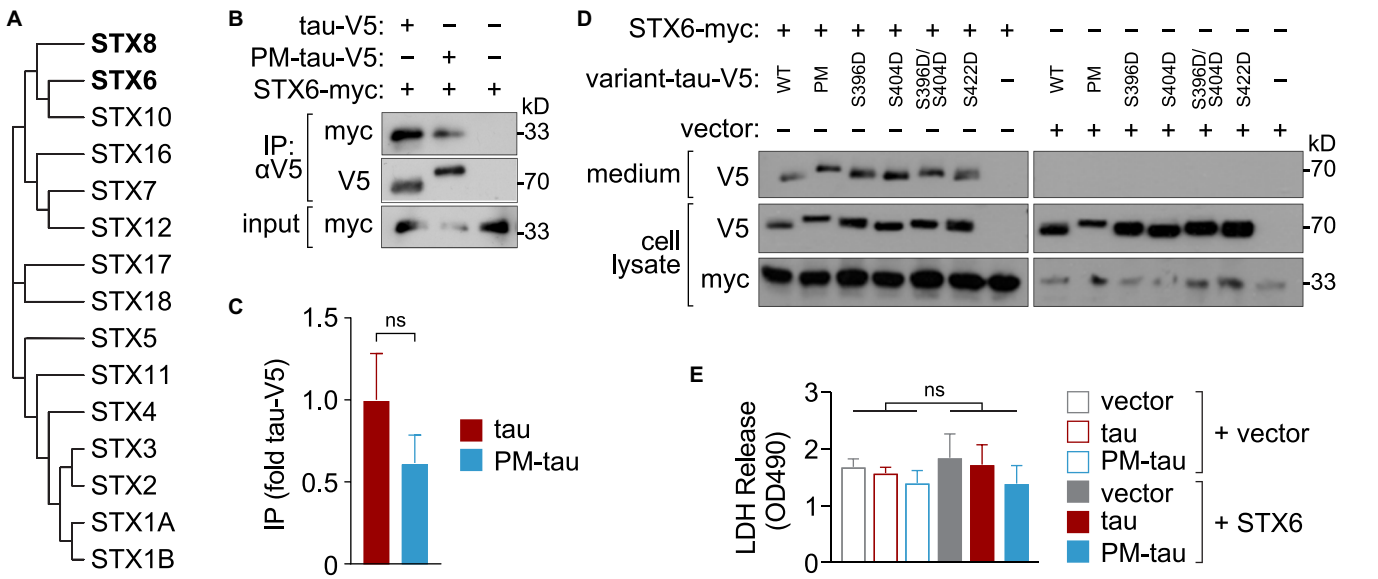


**Figure 4. STX6-mediated tau secretion.**

(**A**) The syntaxin (STX) gene family. (**B**) Co-immunoprecipitation (IP) of myc-tagged STX6 and V5-tagged non-mutant tau or PM-tau (S396D/S404D/S409D/S422D) from transfected cells using V5 antibodies (αV5). (**C**) Quantification of independent IP experiments shown in **B** ($n = 3$; ns, not significant; Student's *t*-test). (**D**) Tau variants, non-mutant (WT), PM and individual/double site phosphorylation-mimicking, appeared only in culture medium with concomitant lower intracellular levels in cells co-transfected with STX6, but not when co-transfected with a myc-vector control. (**E**) Cells expressing non-mutant tau or PM-tau together with or without STX6 show comparable cell viability ($n = 3$; ns, not significant [Student's *t*-test]).

directed mutagenesis to generated the following variants of the 255 amino acid (aa) full-length STX6; aa1–235 (deletion of the transmembrane protein), aa236–255 (transmembrane only), aa1–161 (H1 domain and linker sequence), aa162–255 (H2-snare and transmembrane domains), aa1–71 (H1 domain) and aa72–255 (deletion of the H1 domain). All variants were tagged with a N-terminal enhanced green fluorescence protein (eGFP) sequence. Individual variants were co-transfected with non-mutant tau or PM-tau in 293T cells, and release of tau was determined by precipitating from the culture medium while expression was confirmed in cell lysates (Figure 5A). All STX6 variants that contained the transmembrane domain, including the variant that comprised only the transmembrane domain, resulted in the release of tau into the culture medium, while there was no tau present in the medium when variants that lacked the transmembrane domain were co-expressed. Levels of tau release between transmembrane containing variants were comparable to full-length STX6. For comparison, PM-tau was also released by those STX6 variants that included the transmembrane domain. Given the importance of the STX6 transmembrane domain for the secretion of tau, we next determined the subcellular distribution of the STX6 variants as a possible explanation for their differential effects on non-mutant tau and or PM-tau. Therefore, the subcellular distribution of the eGFP tag was visualized in cells transfected with individual STX6 variants (Figure 5B). Consistent with the previously reported localization of STX6 to the trans-Golgi network, full-length eGFP-tagged STX6 accumulated in perinuclear vesicular structures. Similarly, all variants that included the transmembrane domain showed the same localization as full-length STX6. This included the transmembrane only variants of STX6. In contrast, all variants that lacked the transmembrane domain showed diffuse cytoplasmic distribution, consistent with disrupted targeting to the trans-Golgi network. When expressed in neurons, eGFP-tagged STX6 localized to vesicular intracellular structures, where it colocalized with tau as shown by confocal microscopy with Pearson correlation coefficients (PCC) of 0.47 ± 0.07 (STX6:tau; $n = 4$) indicative of robust co-localization with tau (Figure 5C). Finally, we devised experiments to determine the role of the STX6/8 TM domains in tau secretion directly. Therefore, we tested whether tau could bind synthetic peptides that resemble the sequence of STX6/8 TM domains. When incubated at equimolar concentrations, full-length recombinant tau captured STX6 and STX8 TM domain peptides virtually completely, while the unrelated TM sequence of the RAMP1 protein (=control TM) remained largely unbound

*Biochemical Journal* (2021) **478** 1471–1484
https://doi.org/10.1042/BCJ20200664

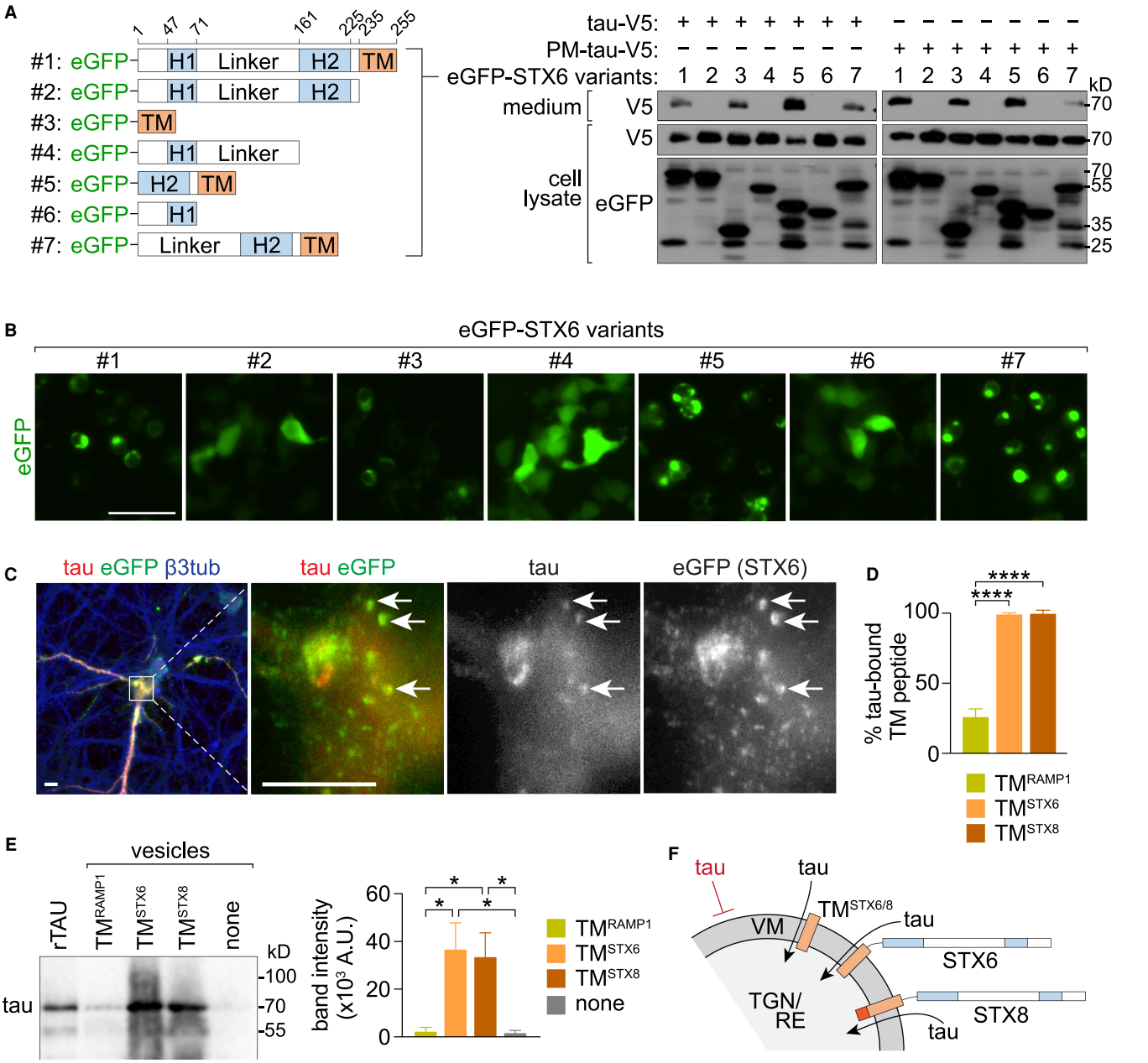


**Figure 5. STX6 transmembrane domain mediates tau secretion.**

(**A**) Illustration (left) of eGFP-tagged STX6 domain structure (#1) and 6 truncation variants (#2–7) used for transfection of cells together with non-mutant tau or PM-tau (right). Only variants containing the C-terminal transmembrane domain (TM) mediated release of non-mutant tau and PM-tau intro the culture medium. (**B**) Representative eGFP fluorescence images of cells transfected with STX6 variants #1–7 show perinuclear accumulation only when variant harbor the TM. (**C**) Representative immunostaining of primary mouse neurons transfected with eGFP-STX6 (green) and human V5-tau (red) together with structural β3-tubulin (β3tub; blue) (*left*). High magnification images show co-localization of V5-tau and eGFP-STX6 in vesicles (arrows) (*overlay* and *individual monochrome channels*). Scale bars, 10 μm. (**D**) Percentage of TM peptides bound to recombinant tau *in vitro* showing virtual complete binding of STX6 and STX8 TM peptide as compared with the control TM (RAMP1) ($n = 9$; **** $P < 0.0001$; Student's *t*-test). (**E**) Recombinant tau (rTAU) protected from trypsinization inside reconstituted bi-lipid vesicles containing STX6 and STX8 TM peptides, while the control TM (RAMP1) fails to transfer tau from outside into vesicles. Quantification from independent experiments ($n = 5$; * $P < 0.05$; Student's *t*-test). (**F**) Illustration of proposed transmembrane transfer of tau via STX6/8 TM, STX6 or STX8 into the trans-Golgi network (TGN) or recycling endosomes (RE) for subsequent secretion.

*Biochemical Journal* (2021) **478** 1471–1484
https://doi.org/10.1042/BCJ20200664

(Figure 5D). Then, we addressed whether the STX6/8 TM domain peptides facilitate transfer of tau across the bi-lipid membrane of reconstituted vesicles *in vitro* and protect them from extravesicular trypsinization. Trypsin-protected full-length tau in vesicles containing synthetic STX6 and STX8 TM domain peptides suggested uptake of tau into vesicles (Figure 5E). In contrast, vesicles with the control TM peptide or vesicles without TM peptides failed to protect tau. Taken together, we showed that the transmembrane domains of STX6 and STX8 bind tau and facilitate its localization across lipid membrane (Figure 5F) as a prerequisite for entry into the secretory network of cells (Supplementary Figure S2).

# Discussion

In the present study, we established a novel interactome of the tau's CTTR using yeast-two-hybrid screening of a human brain cDNA library. This revealed a network of interactors that annotated to distinct cellular pathways. Furthermore, we showed that the novel tau's CTTR interactor STX8 and its closely related family member STX6 mediates the secretion of tau in a cell culture model.

The functional relevance of tau's CTTR had not been explored in detail. It harbors some sites that are known to become phosphorylated late in disease and are closely related to NFT formation [26]. Here, we used a combination of non-mutant CTTR and a variant that contained four of the most widely studied late serine sites mutated to phosphorylation-mimicking aspartic acids to establish a comprehensive interactome of the CTTR. We found that the CTTR mediates interaction with a variety of previously unknown partner proteins when screening a human brain cDNA library. Notably, a prominent cluster of proteins emerged amongst the candidates; interconnected factors that have been linked to the ubiquitin-proteasome and molecular chaperone systems. Hence, the CTTR may play a critical role in the folding and degradation of tau. Furthermore, several interactors were associated with DNA repair, possibly linking to nuclear functions of tau [27,28]. These functions may be compromised in disease by hyperphosphorylation of the CTTR and upon C-terminal truncation [29]. Interestingly, WDR48 interacted less with PM-tau, while PCNA, CUL1, COPS5, HSPA5 and AHSA1 formed similar complexes with non-mutant tau and PM-tau. This suggests that phosphorylation within the CTTR regulates interactions in a partner-specific manner.

C-terminal fragments of tau have been linked to the spreading of pathology [30]. Using a cellular assay for tau release, we show that STX8 is sufficient to facilitate the release of tau from cells, suggesting a new molecular mechanism for tau secretion that involves interaction with STX8 and the endosome/Golgi network. STX8 is a member of the large SNARE class protein family of syntaxins that have diverse functions in secretory pathways (Figure 4A and Supplementary Figure S2) [31]. Accordingly, STX8 localizes to recycling and late endosomes, while the closely related STX6 from this family localizes to the trans-Golgi network and early endosomes [32]. Fittingly, we found co-localization of tau with STX6 in vesicles in cultured neurons. Moreover, STX6 has been linked to increased risk for the tauopathy PSP [24,25]. This suggested that STX6, like STX8, may be involved in pathways that facilitate tau release from cells and thereby contribute to the spreading of tau pathology. Like for STX8, we demonstrate that the TM of STX6 alone can mediate the release of tau from cells. Alignment of TM amino acid sequences of the syntaxin family members revealed similarities and high content of Isoleucine, Leucine and Valine residues that warrant further studies addressing other syntaxins in the context of tau pathology (Supplementary Figure S3). Given the distinct roles of syntaxins in different secretory pathways but similar release of tau facilitated by the TMs of STX6 and STX8, we propose that syntaxins mediate secretion of tau by inserting it into the secretory machinery at different levels of active pathways. This is also in line with depolarization-mediated secretion of tau in mice [33].

In summary, in addition to establishing a new interactome of the tau CTTR that links to tau degradation and folding, we revealed a novel molecular mechanism of tau secretion. This was linked to the molecular function of syntaxins, including STX6 that was previously identified as a risk factor for PSP [24,25]. Whether the tau secretory activity of STX6 contributes to disease onset and progression *in vivo* remains to be shown.

# Materials and methods

## Yeast-two-hybrid screening

Screening was done as previously published by us [34]. Unless specified otherwise, all the reagents and kits for Y2H screening were obtained from Clontech Laboratories, Inc and were used according to the instructions from the Yeast Protocols Handbook and Matchmaker$^{TM}$ Gold Yeast-Two-Hybrid System User Manual (Clontech Laboratories, Inc.). The coding sequences for the CTTR of non-mutant tau or PM-tau were cloned

into the pGBKT7–53 bait plasmid. *Saccharomyces cerevisiae* strain AH109 was transformed with the bait plasmids using lithium acetate (LiAc)-mediated method. Firstly, 5 ml of yeast extract peptone dextrose (YPD) medium was inoculated with a colony (2–3 mm in diameter) freshly grown on agar plate and incubated overnight at 30°C while shaking at 200 rpm. The number of yeast cells in the overnight culture was counted and equalized to a cell density of $5 \times 10^6$ cells/ml with YDP medium and further incubated to a final cell density of $2 \times 10^7$ cells/ml. Yeast was pelleted by centrifugation at 1000×***g*** for 10 min and washed once with sterile water and eventually resuspended in 1 ml of sterile water. Ana amount of 100 ng of plasmid DNA, 36 μl of 1 M LiAc, 240 μl of 50% (w/v) PEG-3350, 10 μl of pre-boiled salmon sperm DNA in a final volume of 360 μl was added to 100 μl of the yeast suspension. The transformation mixture was then incubated for 30 min at 30°C and subjected to a heat shock at 42 °C for 20 min. After centrifugation at 8000 rpm for 30 s, the pellet was resuspended in 500 μl of sterile water and plated on synthetically defined (SD) agar plates lacking tryptophan (SD-Trp) to select for the yeast cells successfully transformed with pGBKT7–53. The plates were incubated until colonies appeared, generally within 2 to 4 days. To identify putative interaction partners, fresh colonies (2–3 mm diameter) transformed with the pGBKT7–53 bait plasmids were inoculated into 50 ml of SD-Trp and incubated overnight at 30°C while shaking at 250 rpm until an $OD_{600}$ of 0.8. Cultures were then centrifuged at 1000×***g*** for 5 min and the pellet resuspended in SD-Trp to a cell density of $1 \times 10^8$ cells/ml. The following day, the bait strain culture was combined with a 1 ml aliquot of the *Saccharomyces cerevisiae* strain Y187 prey strain culture constituted of the Mate & Plate™ Human Brain (Normalized) complementary DNA (cDNA) library (Cat No. 630486) that was pretransformed with pGADT7 prey plasmids containing cDNA inserts from the library. An amount of 45 μl of 2× YPD medium supplemented with adenine hemisulfate (YPDA) and 50 μg/ml kanamycin was added to the cultures and incubated at 30°C for 20 to 24 h whilst slowly shaking at 30–50 rpm for the yeast mating to take place. Once zygotes with a three-lobed structure indicative of two haploid parental cells and a budding haploid cells were observed under a phase-contrast microscope, the culture was centrifuged at 1000×***g*** for 10 min and the pellet was resuspended in 10 ml of 0.5× YPDA supplemented with 50 μg/ml kanamycin. The mated culture was then distributed evenly over 15 cm SD agar plates lacking Adenine (-Ade), Histidine (-His), Leucine (-Leu) and tryptophan (-Trp), designated as quadruple dropout (QDO) agar plates and incubated at 30°C for 4–7 days. All colonies that grew on QDO agar plates were patched out onto higher stringency QDO agar plates supplemented with X-α-galactosidase and Aureobasidin A (QDO/X/A). Every single blue-coloured colony grew on QDO/X/A was subjected to pGADT7 prey plasmid rescue; Colonies were inoculated into 2 ml of QDO medium and incubated overnight at 30°C while shaking at 250 rpm. For DNA extraction, cultures were centrifuged at 1000×***g*** for 10 min and pellets were resuspended in 200 μl of lysis buffer (10 mM of Tris–HCl (pH 8), 1 mM of ethylenediaminetetraacetic acid (EDTA, pH 8), 2% (v/v) of Triton X-100, 1% (w/v) of sodium dodecyl Sulfate (SDS) and 100 mM of sodium chloride (NaCl)). 200 μl of phenol/chloroform/isoamyl alcohol, 25 : 24 : 1 (v/v/v) and 150 μl of acid-washed glass beads (425–600 μm, Cat No. G-8772, Sigma–Aldrich) were added to the cell suspension. The cell suspension was then vortexed at the top speed for 2 min to break up the yeast cells and centrifuged at 14 000 rpm for 5 min to collect the aqueous phase (top layer) containing released DNA. DNA was purified by standard ethanol precipitation. Prey plasmids rescued from the yeast was transformed into electrocompetent DH5α *E.coli* cells (NEB) using high-efficiency electroporation following the manufacturer's protocol. Single bacterial colonies grown on the agar plates were subjected to colony PCR consisting of a primer pair flanking the multiple cloning site of the pGADT7 prey plasmids: T7 Sequencing Forward Primer and 3′ AD Sequencing Reverse Primer. Once the presence of insert was confirmed by the colony PCR, plasmid DNA was extracted from positive clones and sent for sequencing (Macrogen, Korea). Genetic identities of putative protein partners were determined through sequence homology searches to the GenBank sequence data bank with the Nucleotide-nucleotide Basic Local Alignment Search Tool (BLASTn; NCBI). The sequences and functional information of the protein partners were obtained from the UniProt Knowledgebase (UniProtKB) protein database provided by the UniProt consortium. Protein–protein interaction networks were retrieved from Search Tool for the Retrieval of Interacting Genes/Proteins (STRING) version 10.5.

## Plasmids

Human tau plasmids have been previously generated and described [35]. S396, S404, S409 and S422 (according to 2N4R tau) were mutated to aspartic acid (phosphomimetic tau, PM-tau) using Q5 site-directed mutagenesis (New England Biolabs, (NEB)). The open reading frames (ORFs) of interaction candidates from yeast two-hybrid screening were PCR amplified from human cell lines cDNA libraries isolated from SH-SY5Y, HEK293T,

Biochemical Journal (2021) 478 1471–1484
https://doi.org/10.1042/BCJ20200664

U87MG and HS683 cells (ATCC). The amplified transcripts were first cloned into Gateway pENTR-SD-D-TOPO entry vector (Life Technologies), and further transferred into a pcDNA3.2-myc destination vector through LR recombination (Life Technologies). Mammalian expression constructs for V5 tagged tau and PM-tau were generated by LR recombination reaction into pcDNA3.2/V5-DEST vector (Life Technologies). For conventional cloning, PCR primers included restriction sites compatible with the cloning site of target vectors. Amplified products were cut with specific restriction enzymes (NEB) and ligated in-frame into pEGFP-C1 or pDNA3.1 vectors. All cloning primers are listed in Supplementary Table S3.

## Cell culture

Human embryonic kidney (HEK) 293T cells (ATCC) were cultured in HEK media (high glucose Dulbecco's Modified Eagle Media (DMEM,Gibco) supplemented with 10% (v/v) heat-inactivated fetal bovine serum (FBS, Gibco), 2 mM L-glutamine, 1% penicillin and streptomycin (pen/strep, Gibco)) in a humidified 37°C/5% $CO_2$ incubator. Transient transfection of plasmids was done with Polyethylenimine (PEI) at a 3 : 1 ratio mass of PEI to DNA (w/w) [36]. Primary neurons from embryo brains at embryonal day 16 (E16) of C57Bl/6 mice were cultured at a density of 70 000 cells per coverslip as previously descirbed by us [37]. Briefly, after removing the brains from E16.5 mouse embryos and isolating hippocampi with micro-scissors, the dissected hippocampi were placed in 2 ml of ice-cold HBSS. This was followed by the addition of 250 µl of Trypsin (Sigma–Aldrich) and incubation at 37°C for 20 min. Next, 250 µl of Deoxyribonuclease I (DNase I, Sigma–Aldrich) was added for 30 s followed by the addition of 10 ml DMEM (Life Technologies) containing 10% fetal bovine serum (DMEM/10% FBS, Hyclone). After tissue had settled in the bottom of the tube, the supernatant was removed and replaced with fresh 10 ml DMEM/10% FBS to ensure thorough washing of the tissue and removal of any remaining DNaseI. The tissue was then triturated in 1 ml DMEM/10% FBS, using fire-polished Pasteur pipettes to achieve a single cell suspension. Cells were plated on poly-D-Lysine-coated 13 mm round glass coverslips at a density of 70 000 cells per well in a 24 well-plate and incubated at 37°C and 5% $CO_2$ for 1.5 h in DMEM/10% FBS culture medium. After incubation, the medium was replaced with 500 µl per well of complete Neurobasal medium (NB/B27: Neurobasal, Life Technologies; supplemented with 2% B27, Life Technologies + 0.25% GlutaMAX, Invitrogen). Cultures were maintained at at 37°C and 5% $CO_2$ until fixation with 4% paraformaldehyde at 17 DIV. Neurons were transfected with V5-hTau and either eGFP-STX6 at 0 DIV during cell plating, using lipofectamine 3000 (Thermo Fisher Scientific), according to manufacturer's protocol. The medium was changed to NB/B27 at 1.5 h after transfection.

## Co-immunoprecipitation

293T cells were washed twice with ice-cold 1× PBS and harvested by scraping in NP-40 lysis buffer (50 mM of Tris–HCl (pH 8), 150 mM NaCl and 1% (v/v) NP-40 supplemented with 1× Complete protease inhibitor cocktail (Roche)). The cell lysates were incubated in 4°C for 30 min whilst rotating and the supernatant was collected after centrifugation at 21 000×***g*** for 10 min at 4°C. The concentration of protein lysates was measured using the Bio-Rad DC Protein Assay according to the manufacturer's protocol. Co-immunoprecipitation was done as previously reported [36]. Briefly, 293T cells lysates were incubated with one of the following antibodies: mouse anti-V5 (Life Technologies, Cat No. R960CUS), mouse anti-haemagglutinin tag (HA tag) (Sigma–Aldrich, Cat No. H9658) or rabbit anti-HA (Cell Signaling Technology, Cat No. 3724) at 4°C for 16 h whilst rotating. The following day, 25 µl of washed protein G-coupled magnetic Dynabeads™ (Life Technologies) were added to the cell lysates/antibody mixture and incubated for 1 h at 4°C whilst rotating. The lysates were washed three times with NP-40 lysis buffer using the DynaMag magnetic stand to remove any unbound proteins. Bound proteins were eluted with 4× sample buffer (1 M of Tris–HCl (pH 8), 9.2% (w/v) SDS, 40% (v/v) glycerol, 20% (v/v) β-mercaptoethanol and 0.2% (w/v) bromophenol blue) and separated by SDS–PAGE. Western blotting was done as previously described [36]. Primary antibodies were: anti-V5 conjugated with horseradish peroxidase (hrp) (V5-HRP) (Life Technologies, Cat No. R961–25, 1:5000 in 3% (w/v) BSA in TBST), anti-myc conjugated with HRP (myc-HRP) (Life Technologies, Cat No. R951–25, 1 : 5000), mouse anti-HA-tag (Sigma–Aldrich, Cat No. H9658, 1 : 1000) and rabbit anti-HA-tag (Cell Signaling Technology, Cat No. 3724, 1 : 1000).

## Tau release assay

293T cells were co-transfected with either WT-tau or PM-tau constructs (tagged with V5) together with expression plasmids for interaction candidates or an empty pcDNA3 vector control. Seventy-two hours after

transfection medium was collected and cells harvested. Media were centrifuged at 5000×*g*, 4°C for 10 min to pellet any floating cells. Anti-v5 antibody was added to media supernatants and rotated for 16 to 18 h at 4°C. Supernatants were then incubated with magnetic beads, washed and eluted with sample buffer for SDS–PAGE.

## Cell viability assay

Cell viability was measured with the CytoTox 96® Non-Radioactive Cytotoxicity Assay (Promega) that determined the amount of lactate dehydrogenase (LDH) in media as per manufacturer's instructions.

## Cell staining

GFP localization was visualized in life 293T cells using an inverted fluorescence microscope (Zeiss). Neurons were fixed at 17 DIV with 4% paraformaldehyde for 15 min at room temperature (RT), then permeabilised using 0.1% tritonX100 (Sigma–Aldrich) for 5 min at RT. After washing twice with PBS, cells were blocked in PBS containing 2% FBS for 30 min at RT followed by incubation with primary antibodies at 4°C overnight. The next day, coverslips were washed five times in PBS, then incubated with secondary antibody for 30 min at room temperature. Coverslips were again washed five times in PBS and then mounted onto glass slides using mounting medium (DAKO). All primary and secondary antibodies were diluted in PBS containing 2% FBS and they include the following: rabbit GFP (1 : 1000; Abcam ab290), mouse Tau13 (1 : 500; Santa Cruz sc-21796), chicken β3-Tubulin (1 : 300; Milipore ab9354), donkey anti-rabbit Alexa-488 (1 : 500; Life Technologies A32790), donkey anti-mouse Alexa-555 (1 : 500; Life Technologies A31570), goat anti-chicken Alexa-647 (1 : 500; Life Technologies, A21449), DAPI (1 : 1000, Life Technologies D1306). Neurons were imaged as *z*-stacks at intervals of 0.25 μm using an inverted Zeiss LSM880 Confocal microscope with a plan-apochromatic 63×/1.4 oil DIC M27 objective. Somatic regions of interest were acquired using a 2× zoom. To quantify the association of tau with STX6, image analysis was performed on single *z*-stack images of transfected hippocampal somas using the EzColocalization plugin in ImageJ software (v.2.1.0). Pearson's correlation coefficient (PCC) was measured in a selected region of interest within the soma of a transfected cell. The range of the area measured was between 40 and 140 $\mu m^2$. PCC was determined between 555 nm (human tau) channel 488 nm (STX6) channel. Four cells were analyzed for colocalization of STX6 with Tau.

## Peptide synthesis

Peptides with the amino acid sequence of the transmembrane domains of STX6, STX8 and RAMP1 were synthesized in-house using automated microwave-assisted solid-phase peptide synthesis (CEM) and purified under reverse phase HPLC (Hamamatsu) conditions to give a final peptide purity of >95% in all cases.

## *In vitro* TM interaction assay

TM peptides were mixed individually with full-length recombinant tau (hTau) at a 1 : 1 ratio (10 μM TM peptide and 10 μM hTau) in PBS. The mixtures were incubated at 4°C, room temperature or 37°C for 1 h while rotating slowly. An amount of 30 μl of each mixture were used for liquid chromatography–mass spectrometry (LC–MS). LC–MS was done with a Shimazu LC–MS 8050 equipment, using product ion scan with a cut-off of 2000 kD to measure unbound peptides. Ion mass was set to mass of the individual peptides. Area under the curve (AUC) analysis of peptide peaks was done for quantification. Baseline LC–MS signals were determined by measuring samples containing recombinant tau but no TM peptides. All readings were background corrected and normalized to AUC data from 30 μl of 10 μM of each TM peptide (=maximum free/unbound peptide). All experiments were repeated three times for each incubation temperature. Since there was no overt difference between incubation temperatures, data was pooled. Values are presented as percentage of bound peptide.

## *In vitro* tau protection assay

Artificial bi-lipid membrane vesicles (liposomes) were generated in the presence or absence of individual TM peptides. The preparation of liposomes was performed by following the manufacturer's instructions (Sigma–Aldrich L4395). Briefly, TM peptides were dissolved in dimethyl sulfoxide (Sigma) at 1.849 mM. 10 μM of peptide or solvent were each added to 0.19 ml phosphate-buffered saline (PBS) and transferred into individual vials with dry lipid film for reconstitution of liposomes. After vortexing, 0.8 ml PBS was added to each vial followed by 30 min of agitation at room temperature to complete vesicle formation. Full-length recombinant tau (2N4R) was added to each vial to a final concentration of 90 μM and incubated at 37°C for 24 h. Tau outside

*Biochemical Journal* (2021) **478** 1471–1484
https://doi.org/10.1042/BCJ20200664

of vesicles was digested by incubation with trypsin (Invitrogen) at 37°C for 10 min before analysis by Western blotting.

## Protein alignment

Amino acid sequences constituting the transmembrane domains of each syntaxin were obtained from https://www.uniprot.org/. No data was available for human STX11, and STX17 was the only syntaxin with two TMs. Sequence alignments of TM sequences was done with CLUSTAL O(1.2.4) followed by the manual highlighting of similar and homolog residues.

## Statistical analysis

Statistical analysis was done with the Prism software (GraphPad). Student's *t*-tests were used to determine statistical significance. $P$ values of $<0.05$ were considered significant. All values were presented as mean ± standard error of mean (SEM).

### Competing Interests

The authors declare that there are no competing interests associated with the manuscript.

### Funding

This research was supported by funding from the National Health and Medical Research Council (NHMRC) (#1081916, #1132524, #1143848, #1143978, #2000660), the Australian Research Council (#DP150104321, #DP170100781, #DP170100843) and Macquarie University. Y.K. is a NHMRC Career Development Fellow (#1123564). L.I. is a NHMRC Principal Research Fellow (#1136241).

### Open Access

Open access for this article was enabled by the participation of Macquarie University in an all-inclusive *Read & Publish* pilot with Portland Press and the Biochemical Society under a transformative agreement with CAUL.

### CRediT Contribution

**Lars M. Ittner:** Conceptualization, Supervision, Funding acquisition, Visualization, Writing — original draft, Project administration. **Wei Siang Lee:** Data curation, Formal analysis, Methodology, Writing — review and editing. **Daniel CS Tan:** Data curation, Formal analysis, Methodology, Writing — review and editing. **Yuanyuan Deng:** Formal analysis, Methodology, Writing — review and editing. **Annika van Hummel:** Formal analysis, Writing — review and editing. **Stefania Ippati:** Formal analysis, Writing — review and editing. **Claire Stevens:** Formal analysis, Writing — review and editing. **Paulina Carmona-Mora:** Data curation, Formal analysis, Writing — review and editing. **Daryl Ariawan:** Data curation, Methodology, Writing — review and editing. **Liming Hou:** Data curation, Methodology, Writing — review and editing. **Holly Stefen:** Data curation, Formal analysis, Writing — review and editing. **Tamara Tomanic:** Data curation, Writing — review and editing. **Mian Bi:** Formal analysis, Writing — review and editing. **Florence Tomasetig:** Data curation, Writing — review and editing. **Adam Martin:** Formal analysis, Writing — review and editing. **Thomas Fath:** Formal analysis, Supervision, Funding acquisition, Project administration, Writing — review and editing. **Stephen Palmer:** Supervision, Funding acquisition, Writing — review and editing. **Yazi D. Ke:** Conceptualization, Supervision, Funding acquisition, Writing — original draft, Project administration.

### Acknowledgements

The authors thank the staff off the Macquarie Animal Research Service for expert animal care.

### Abbreviations

AD, Alzheimer's disease; AHSA1, activator of 90 kDa heat shock protein ATPase; AUC, area under the curve; CNRIP1, CB1 cannabinoid receptor-interacting protein 1; CTTR, C-terminal tail region; CUL1, cullin-1; FBS, fetal bovine serum; HEK, human embryonic kidney; HRP, horseradish peroxidase; LDH, lactate dehydrogenase; NFT, neurofibrillary tangle; PCNA, proliferating cell nuclear antigen; PSP, progressive supranuclear palsy; QDO, quadruple dropout; SDS, sodium dodecyl Sulfate; STX6, syntaxin 6; WDR48, WD repeat-containing protein 48; YPD, yeast extract peptone dextrose.

## References


1 Ittner, A. and Ittner, L.M. (2018) Dendritic tau in Alzheimer's disease. *Neuron* **99**, 13–27 https://doi.org/10.1016/j.neuron.2018.06.003
2 Kempf, M., Clement, A., Faissner, A., Lee, G. and Brandt, R. (1996) Tau binds to the distal axon early in development of polarity in a microtubule- and microfilament-dependent manner. *J. Neurosci.* **16**, 5583–5592 https://doi.org/10.1523/JNEUROSCI.16-18-05583.1996
3 Buee, L., Bussiere, T., Buee-Scherrer, V., Delacourte, A. and Hof, P.R. (2000) Tau protein isoforms, phosphorylation and role in neurodegenerative disorders. *Brain Res. Brain Res. Rev.* **33**, 95–130 https://doi.org/10.1016/S0165-0173(00)00019-9
4 Ballatore, C., Lee, V.M. and Trojanowski, J.Q. (2007) Tau-mediated neurodegeneration in Alzheimer's disease and related disorders. *Nat. Rev. Neurosci.* **8**, 663–672 https://doi.org/10.1038/nrn2194
5 Goedert, M., Spillantini, M.G., Cairns, N.J. and Crowther, R.A. (1992) Tau proteins of Alzheimer paired helical filaments: abnormal phosphorylation of all six brain isoforms. *Neuron* **8**, 159–168 https://doi.org/10.1016/0896-6273(92)90117-V
6 Grundke-Iqbal, I., Iqbal, K., Quinlan, M., Tung, Y.C., Zaidi, M.S. and Wisniewski, H.M. (1986) Microtubule-associated protein tau. A component of Alzheimer paired helical filaments. *J. Biol. Chem.* **261**, 6084–6089 https://doi.org/10.1016/S0021-9258(17)38495-8
7 Goedert, M., Spillantini, M.G., Jakes, R., Rutherford, D. and Crowther, R.A. (1989) Multiple isoforms of human microtubule-associated protein tau: sequences and localization in neurofibrillary tangles of Alzheimer's disease. *Neuron* **3**, 519–526 https://doi.org/10.1016/0896-6273(89)90210-9
8 Hirokawa, N., Shiomura, Y. and Okabe, S. (1988) Tau proteins: the molecular structure and mode of binding on microtubules. *J. Cell Biol.* **107**, 1449–1459 https://doi.org/10.1083/jcb.107.4.1449
9 Crowther, T., Goedert, M. and Wischik, C.M. (1989) The repeat region of microtubule-associated protein tau forms part of the core of the paired helical filament of Alzheimer's disease. *Ann. Med.* **21**, 127–132 https://doi.org/10.3109/07853898909149199
10 Butner, K.A. and Kirschner, M.W. (1991) Tau protein binds to microtubules through a flexible array of distributed weak sites. *J. Cell Biol.* **115**, 717–730 https://doi.org/10.1083/jcb.115.3.717
11 Konzack, S., Thies, E., Marx, A., Mandelkow, E.M. and Mandelkow, E. (2007) Swimming against the tide: mobility of the microtubule-associated protein tau in neurons. *J. Neurosci.* **27**, 9916–9927 https://doi.org/10.1523/JNEUROSCI.0927-07.2007
12 Brandt, R., Leger, J. and Lee, G. (1995) Interaction of tau with the neural plasma membrane mediated by tau's amino-terminal projection domain. *J. Cell Biol.* **131**, 1327–1340 https://doi.org/10.1083/jcb.131.5.1327
13 Magnani, E., Fan, J., Gasparini, L., Golding, M., Williams, M., Schiavo, G. et al. (2007) Interaction of tau protein with the dynactin complex. *EMBO J.* **26**, 4546–4554 https://doi.org/10.1038/sj.emboj.7601878
14 Stefanoska, K., Volkerling, A., Bertz, J., Poljak, A., Ke, Y.D., Ittner, L.M. et al. (2018) An N-terminal motif unique to primate tau enables differential protein-protein interactions. *J. Biol. Chem.* **293**, 3710–3719 https://doi.org/10.1074/jbc.RA118.001784
15 Lee, G., Newman, S.T., Gard, D.L., Band, H. and Panchamoorthy, G. (1998) Tau interacts with src-family non-receptor tyrosine kinases. *J. Cell Sci.* **111**, 3167–3177 PMID:9763511
16 Ittner, L.M., Ke, Y.D., Delerue, F., Bi, M., Gladbach, A., van Eersel, J. et al. (2010) Dendritic function of tau mediates amyloid-beta toxicity in Alzheimer's disease mouse models. *Cell* **142**, 387–397 https://doi.org/10.1016/j.cell.2010.06.036
17 Liu, Z.C., Fu, Z.Q., Song, J., Zhang, J.Y., Wei, Y.P., Chu, J. et al. (2012) Bip enhanced the association of GSK-3beta with tau during ER stress both in vivo and in vitro. *J. Alzheimers Dis.* **29**, 727–740 https://doi.org/10.3233/JAD-2012-111898
18 Prekeris, R., Yang, B., Oorschot, V., Klumperman, J. and Scheller, R.H. (1999) Differential roles of syntaxin 7 and syntaxin 8 in endosomal trafficking. *Mol. Biol. Cell* **10**, 3891–3908 https://doi.org/10.1091/mbc.10.11.3891
19 Bhat, S.S., Friedmann, K.S., Knorck, A., Hoxha, C., Leidinger, P., Backes, C. et al. (2016) Syntaxin 8 is required for efficient lytic granule trafficking in cytotoxic T lymphocytes. *Biochim. Biophys. Acta* **1863**, 1653–1664 https://doi.org/10.1016/j.bbamcr.2016.04.014
20 Goedert, M., Eisenberg, D.S. and Crowther, R.A. (2017) Propagation of tau aggregates and neurodegeneration. *Annu. Rev. Neurosci.* **40**, 189–210 https://doi.org/10.1146/annurev-neuro-072116-031153
21 Fuster-Matanzo, A., Hernandez, F. and Avila, J. (2018) Tau spreading mechanisms; implications for dysfunctional tauopathies. *Int. J. Mol. Sci.* **19**, 645 https://doi.org/10.3390/ijms19030645
22 Gibbons, G.S., Lee, V.M.Y. and Trojanowski, J.Q. (2019) Mechanisms of cell-to-cell transmission of pathological tau: a review. *JAMA Neurol.* **76**, 101–108 https://doi.org/10.1001/jamaneurol.2018.2505
23 Kara, E., Marks, J.D. and Aguzzi, A. (2018) Toxic protein spread in neurodegeneration: reality versus fantasy. *Trends Mol. Med.* **24**, 1007–1020 https://doi.org/10.1016/j.molmed.2018.09.004
24 Hoglinger, G.U., Melhem, N.M., Dickson, D.W., Sleiman, P.M., Wang, L.S., Klei, L. et al. (2011) Identification of common variants influencing risk of the tauopathy progressive supranuclear palsy. *Nat. Genet.* **43**, 699–705 https://doi.org/10.1038/ng.859
25 Ferrari, R., Ryten, M., Simone, R., Trabzuni, D., Nicolaou, N., Hondhamuni, G. et al. (2014) Assessment of common variability and expression quantitative trait loci for genome-wide associations for progressive supranuclear palsy. *Neurobiol. Aging* **35**, 1514 e1–1514 e12 https://doi.org/10.1016/j.neurobiolaging.2014.01.010
26 Bussiere, T., Hof, P.R., Mailliot, C., Brown, C.D., Caillet-Boudin, M.L., Perl, D.P. et al. (1999) Phosphorylated serine422 on tau proteins is a pathological epitope found in several diseases with neurofibrillary degeneration. *Acta Neuropathol.* **97**, 221–230 https://doi.org/10.1007/s004010050978
27 Sultan, A., Nesslany, F., Violet, M., Begard, S., Loyens, A., Talahari, S. et al. (2011) Nuclear tau, a key player in neuronal DNA protection. *J. Biol. Chem.* **286**, 4566–4575 https://doi.org/10.1074/jbc.M110.199976
28 Ke, Y., Dramiga, J., Schutz, U., Kril, J.J., Ittner, L.M., Schroder, H. et al. (2012) Tau-mediated nuclear depletion and cytoplasmic accumulation of SFPQ in Alzheimer's and pick's disease. *PLoS ONE* **7**, e35678 https://doi.org/10.1371/journal.pone.0035678
29 Flores-Rodriguez, P., Ontiveros-Torres, M.A., Cardenas-Aguayo, M.C., Luna-Arias, J.P., Meraz-Rios, M.A., Viramontes-Pintos, A. et al. (2015) The relationship between truncation and phosphorylation at the C-terminus of tau protein in the paired helical filaments of Alzheimer's disease. *Front. Neurosci.* **9**, 33 https://doi.org/10.3389/fnins.2015.00033
30 Matsumoto, S.E., Motoi, Y., Ishiguro, K., Tabira, T., Kametani, F., Hasegawa, M. et al. (2015) The twenty-four KDa C-terminal tau fragment increases with aging in tauopathy mice: implications of prion-like properties. *Hum. Mol. Genet.* **24**, 6403–6416 https://doi.org/10.1093/hmg/ddv351
31 Teng, F.Y., Wang, Y. and Tang, B.L. (2001) The syntaxins. *Genome Biol.* **2**, REVIEWS3012 https://doi.org/10.1186/gb-2001-2-11-reviews3012

*Biochemical Journal* (2021) **478** 1471–1484
https://doi.org/10.1042/BCJ20200664

32 Jung, J.J., Inamdar, S.M., Tiwari, A. and Choudhury, A. (2012) Regulation of intracellular membrane trafficking and cell dynamics by syntaxin-6. *Biosci. Rep.* **32**, 383–391 https://doi.org/10.1042/BSR20120006

33 Yamada, K., Holth, J.K., Liao, F., Stewart, F.R., Mahan, T.E., Jiang, H. et al. (2014) Neuronal activity regulates extracellular tau in vivo. *J. Exp. Med.* **211**, 387–393 https://doi.org/10.1084/jem.20131685

34 Carmona-Mora, P., Widagdo, J., Tomasetig, F., Canales, C.P., Cha, Y., Lee, W. et al. (2015) The nuclear localization pattern and interaction partners of GTF2IRD1 demonstrate a role in chromatin regulation. *Hum. Genet.* **134**, 1099–1115 https://doi.org/10.1007/s00439-015-1591-0

35 Ittner, L.M., Ke, Y.D. and Gotz, J. (2009) Phosphorylated tau interacts with c-Jun N-terminal kinase-interacting protein 1 (JIP1) in Alzheimer disease. *J. Biol. Chem.* **284**, 20909–20916 https://doi.org/10.1074/jbc.M109.014472

36 Ittner, L.M., Koller, D., Muff, R., Fischer, J.A. and Born, W. (2005) The N-terminal extracellular domain 23-60 of the calcitonin receptor-like receptor in chimeras with the parathyroid hormone receptor mediates association with receptor activity-modifying protein 1. *Biochemistry* **44**, 5749–5754 https://doi.org/10.1021/bi048111o

37 Fath, T., Ke, Y.D., Gunning, P., Gotz, J. and Ittner, L.M. (2009) Primary support cultures of hippocampal and substantia nigra neurons. *Nat. Protoc.* **4**, 78–85 https://doi.org/10.1038/nprot.2008.199

## Supplementary Tables

**Table S1. Yeast-two-hybrid interaction candidate hits.** List and frequency of all candidate proteins identified through yeast-two-hybrid (Y2H) with the baits tau-CTTR and PM-tau-CTTR.

| Protein | Description | Entrez Gene ID | Y2H hits/bait | |
|---|---|---|---|---|
| | | | tau-CTTR | PM-tau-CTTR |
| AHSA1 | activator of HSP90 ATPase activity 1 | 10598 | 1 | 0 |
| ANKHD1 | ankyrin repeat and KH domain containing 1 | 54882 | 0 | 1 |
| AP3B2 | adaptor related protein complex 3 subunit beta 2 | 8120 | 0 | 1 |
| ASB12 | ankyrin repeat and SOCS box containing 12 | 142689 | 0 | 1 |
| ATP1B1 | ATPase Na+/K+ transporting subunit beta 1 | 481 | 1 | 2 |
| ATP1B2 | ATPase Na+/K+ transporting subunit beta 2 | 482 | 0 | 2 |
| BBS7 | Bardet-Biedl syndrome 7 | 55212 | 0 | 1 |
| BPGM | bisphosphoglycerate mutase | 669 | 0 | 2 |
| CCDC85A | coiled-coil domain containing 85A | 114800 | 1 | 0 |
| CEP192 | centrosomal protein 192 | 55125 | 1 | 1 |
| CHORDC1 | cysteine and histidine rich domain containing 1 | 26973 | 1 | 0 |
| CKAP5 | cytoskeleton associated protein 5 | 9793 | 3 | 1 |
| CMPK1 | cytidine/uridine monophosphate kinase 1 | 51727 | 3 | 0 |
| CNRIP1 | cannabinoid receptor interacting protein 1 | 25927 | 2 | 3 |
| COMMD8 | COMM domain containing 8 | 54951 | 0 | 1 |
| COPS5 | COP9 signalosome subunit 5 | 10987 | 0 | 8 |
| CUL1 | cullin 1 | 8454 | 0 | 1 |
| DNAJA2 | DnaJ heat shock protein family member A2 | 10294 | 1 | 0 |
| EFR3A | EFR3 homolog A | 23167 | 1 | 0 |
| EIF4A1 | eukaryotic translation initiation factor 4A1 | 1973 | 0 | 1 |
| FARSB | phenylalanyl-tRNA synthetase subunit beta | 10056 | 0 | 1 |
| GFAP | glial fibrillary acidic protein | 2670 | 1 | 0 |
| GFM2 | GTP dependent ribosome recycling factor mitochondrial 2 | 84340 | 1 | 0 |
| HECTD1 | HECT domain E3 ubiquitin protein ligase 1 | 25831 | 2 | 0 |
| HSPA5 | heat shock protein family A member 5 | 3309 | 1 | 2 |
| IL1RAP | interleukin 1 receptor accessory protein | 3556 | 1 | 0 |
| KRT222 | keratin 222 | 125113 | 1 | 2 |
| MYLK | myosin light chain kinase | 4638 | 1 | 0 |
| MYT1L | myelin transcription factor 1 like | 23040 | 0 | 1 |
| N4BP2L2 | NEDD4 binding protein 2 like 2 | 10443 | 0 | 1 |
| NIM1K | NIM1 serine/threonine protein kinase | 167359 | 1 | 0 |
| OMG | oligodendrocyte myelin glycoprotein | 4974 | 1 | 0 |
| PCNA | proliferating cell nuclear antigen | 5111 | 2 | 0 |
| PDE4DIP | phosphodiesterase 4D interacting protein | 9659 | 1 | 1 |
| PGM1 | phosphoglucomutase 1 | 5236 | 1 | 1 |
| PNISR | PNN interacting serine and arginine rich protein | 25957 | 0 | 4 |
| PPP2R3C | protein phosphatase 2 regulatory subunit B"gamma | 55012 | 0 | 1 |
| RPN2 | ribophorin II | 6185 | 1 | 0 |
| SGIP1 | SH3GL interacting endocytic adaptor 1 | 84251 | 0 | 1 |
| SNAPIN | SNAP associated protein | 23557 | 2 | 0 |
| SPOP | speckle type BTB/POZ protein | 8405 | 0 | 3 |
| SRSF5 | serine and arginine rich splicing factor 5 | 6430 | 1 | 0 |
| STX8 | syntaxin 8 | 9482 | 0 | 2 |
| TMEM132B | transmembrane protein 132B | 114795 | 1 | 0 |
| UBE2N | ubiquitin conjugating enzyme E2 N | 7334 | 2 | 0 |
| WDR48 | WD repeat domain 48 | 57599 | 0 | 2 |

**Table S2. STRING functional GO term annotation of CTTR interaction candidates.** GO term annotation of candidate interacting proteins of the tau-CTTR and/or PM-tau-CTTR identified through Y2H and interpreted using the STRING functional enrichment tool. Only terms after a redundancy cutoff of 0.293 were shown. FDR values were obtain through the Benjamini–Hochberg procedure. PPI Enrichment Score: 0.00139

| Category | Term ID | Description | Count | Enriched proteins | FDR value |
|---|---|---|---|---|---|
| GO Function | GO.0031625 | ubiquitin protein ligase binding | 5 | STX8\|UBE2N\|HSPA5\|CUL1\|SPOP | 5.70E-04 |
| GO Function | GO.0051087 | chaperone binding | 3 | AHSA1\|DNAJA2\|HSPA5 | 3.60E-03 |
| GO Function | GO.0051879 | Hsp90 protein binding | 2 | AHSA1\|CHORDC1 | 1.10E-02 |
| GO Process | GO.1903894 | regulation of IRE1-mediated unfolded protein response | 2 | HSPA5\|COPS5 | 1.40E-02 |
| GO Function | GO.0032555 | purine ribonucleotide binding | 6 | EIF4A1\|GFM2\|DNAJA2\|UBE2N\|CHORDC1\|HSPA5 | 2.80E-02 |
| GO Function | GO.0000149 | SNARE binding | 2 | STX8\|SNAPIN | 3.40E-02 |
| GO Process | GO.0006281 | DNA repair | 4 | WDR48\|UBE2N\|COPS5\|PCNA | 4.00E-02 |

**Table S3. Cloning primer sequences.**

| **Gene/Plasmid** | **Primer Sequences** (F, forward; R, reverse) |
|---|---|
| AHSA1 into pENTR-SD-TOPO | F: 5'-CACCATGGCCAAGTGGGGTGAGG<br>R: 5'-AAATAAGCGTGCGCCATAGC |
| CNRIP1 into pENTR-SD-TOPO | F: 5'-CACCATGGGGGACCTGCCGGG<br>R: 5'-GAGGAAGGACTCCTTGTTCA |
| COPS5 into pENTR-SD-TOPO | F: 5'-CACCATGGCGGCGTCCGGGAG<br>R: 5'-AGAGATGTTAATTTGATTAAACAGTT |
| CUL1 into pENTR-SD-TOPO | F: 5'-CACCATGTCGTCAACCCGGAGCC<br>R: 5'-AGCCAAGTAACTGTAGGTGTC |
| HSPA5 into pENTR-SD-TOPO | F: 5'-CACCATGAAGCTCTCCCTGGTGG<br>R: 5'-AGCCAACTCATCTTTTTCTGCTGTA |
| PCNA into pENTR-SD-TOPO | F: 5'-CACCATGTTCGAGGCGCGCCTG<br>R: 5'-AGATCCTTCTTCATCCTCGAT |
| SNAPIN into pENTR-SD-TOPO | F: 5'-CACCATGGCGGGGGCTGGTTCC<br>R: 5'-TTTGCCTGGGGAGCCAGG |
| STX6 into pENTR-SD-TOPO | F: 5'-CACCATGTCCATGGAGGACCCCT<br>R: 5'-CAGCACTAAGAAGAGGATGA |
| STX8 into pENTR-SD-TOPO | F: 5'-CACCATGGCACCGGACCCCTGG<br>R: 5'-GTTGGTCGGCCAGACTGCA |
| WDR48 into pENTR-SD-TOPO | F: 5'-CACCATGGCGGCCCATCACCGG<br>R: 5'-CGTGGACTTCTGACGGTAAT |
| STX8-HA into pcDNA3.1 | F: 5'-TAAGGATCCCACCATGGCACCGGACCCCTGG<br>R: 5'-TGTGAATTCCTAAGCGTAATCTGGAACATCGTATGGGTAGGATCTG<br>TTGGTCGGCCAGACTGCA |
| pEGFPC1-STX6 FL | F: 5'-GGTGAATTCTATGTCCATGGAGGACCCCT<br>R: 5'-TAAGGATCCTCATCACAGCACTAAGAAGAGG |
| pEGFPC1-STX6 1-234 | F: 5'-GGTGAATTCTATGTCCATGGAGGACCCCT<br>R: 5'-TAAGGATCCCTATTGGCGCCGATCACTGGTC |
| pEGFPC1-STX6 235-255 | F: 5'-GGTGAATTCTTGGTGTGCCATAGCCATCC<br>R: 5'-TAAGGATCCTCATCACAGCACTAAGAAGAGG |
| pEGFPC1-STX6 1-160 | F: 5'-GGTGAATTCTATGTCCATGGAGGACCCCT<br>R: 5'-TAAGGATCCTCATGCCTGCTGCTCCTCAATG |
| pEGFPC1-STX6 161-255 | F: 5'-GGTGAATTCTCAGCAGCAGTTGATCGTGG<br>R: 5'-TAAGGATCCTCATGCCTGCTGCTCCTCAATG |
| pEGFPC1-STX6 1-71 | F: 5'-GGTGAATTCTATGTCCATGGAGGACCCCT<br>R: 5'-TAAGGATCCTCAAACTATGCTGATGGTTTCATC |
| pEGFPC1-STX6 72-255 | F: 5'-GGTGAATTCTGAAGCAAATCCTAGAAAATTT<br>R: 5'-TAAGGATCCTCATCACAGCACTAAGAAGAGG |

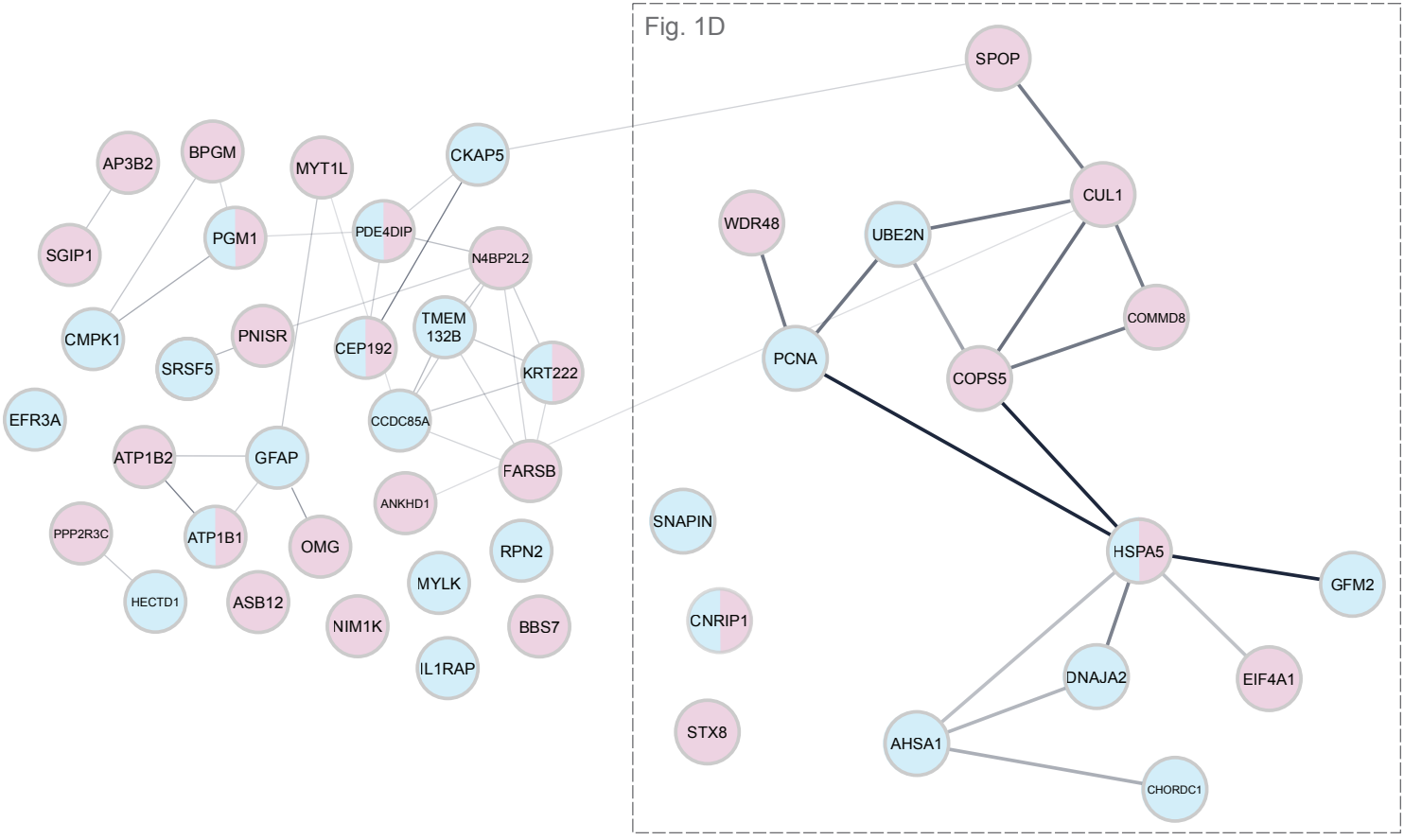


**Fig. S1. Complete STRING networks of CTTR and PM-CTTR interaction candidates.** Ubiquitin-proteasome and molecular chaperons clusters and in individual candidate presented in Fig. 1D are highlighted (broken box).

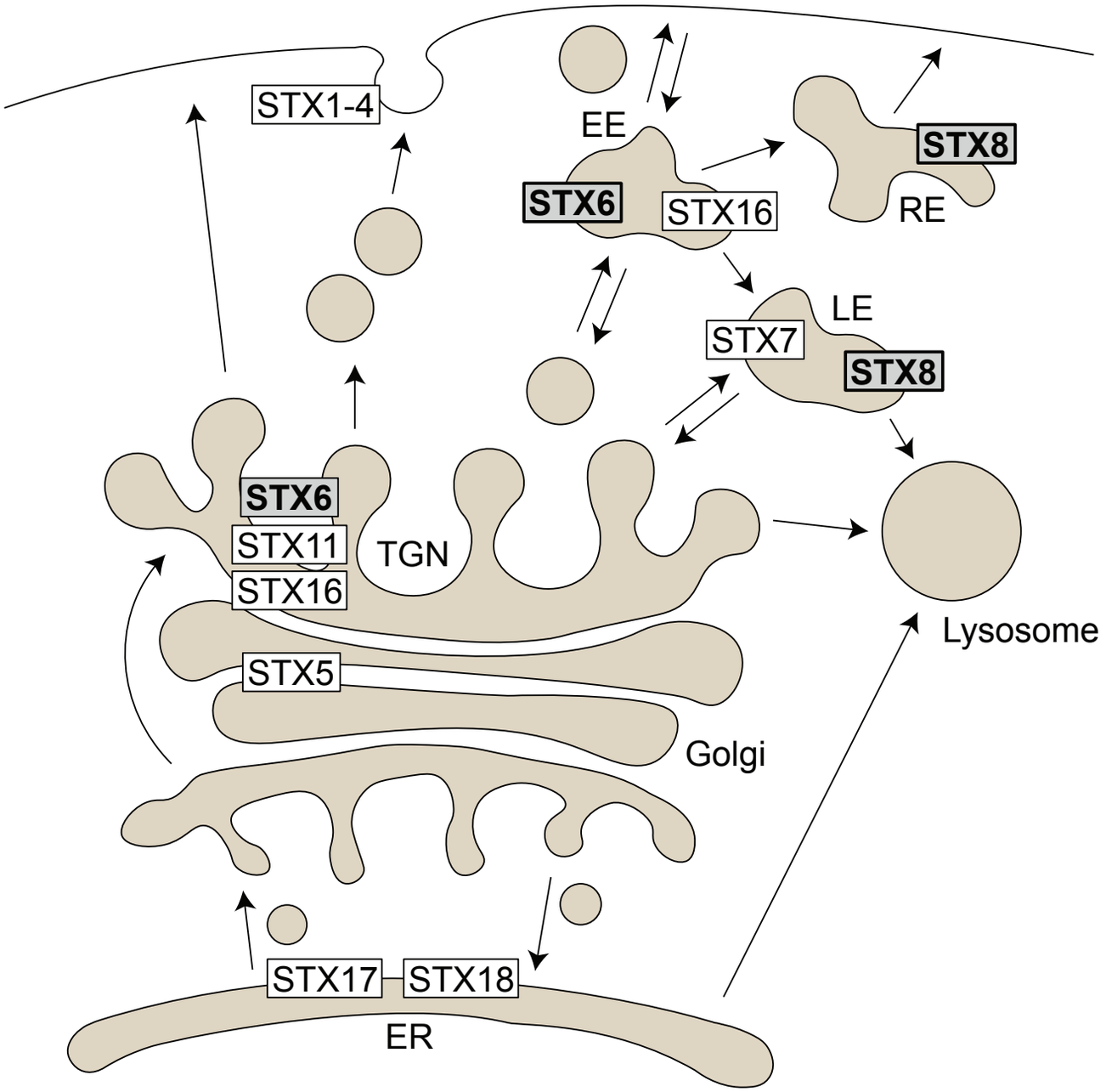


**Fig. S2. Schematic of secretory pathways and syntaxins.** Illustration of the distinct localizations of individual syntaxins (STX) within the secretory machinery of cells. ER, endoplasmic reticulum; TGN, trans-Golgi network; EE, early endosome; LE, late endosome; RE, recycling endosome.

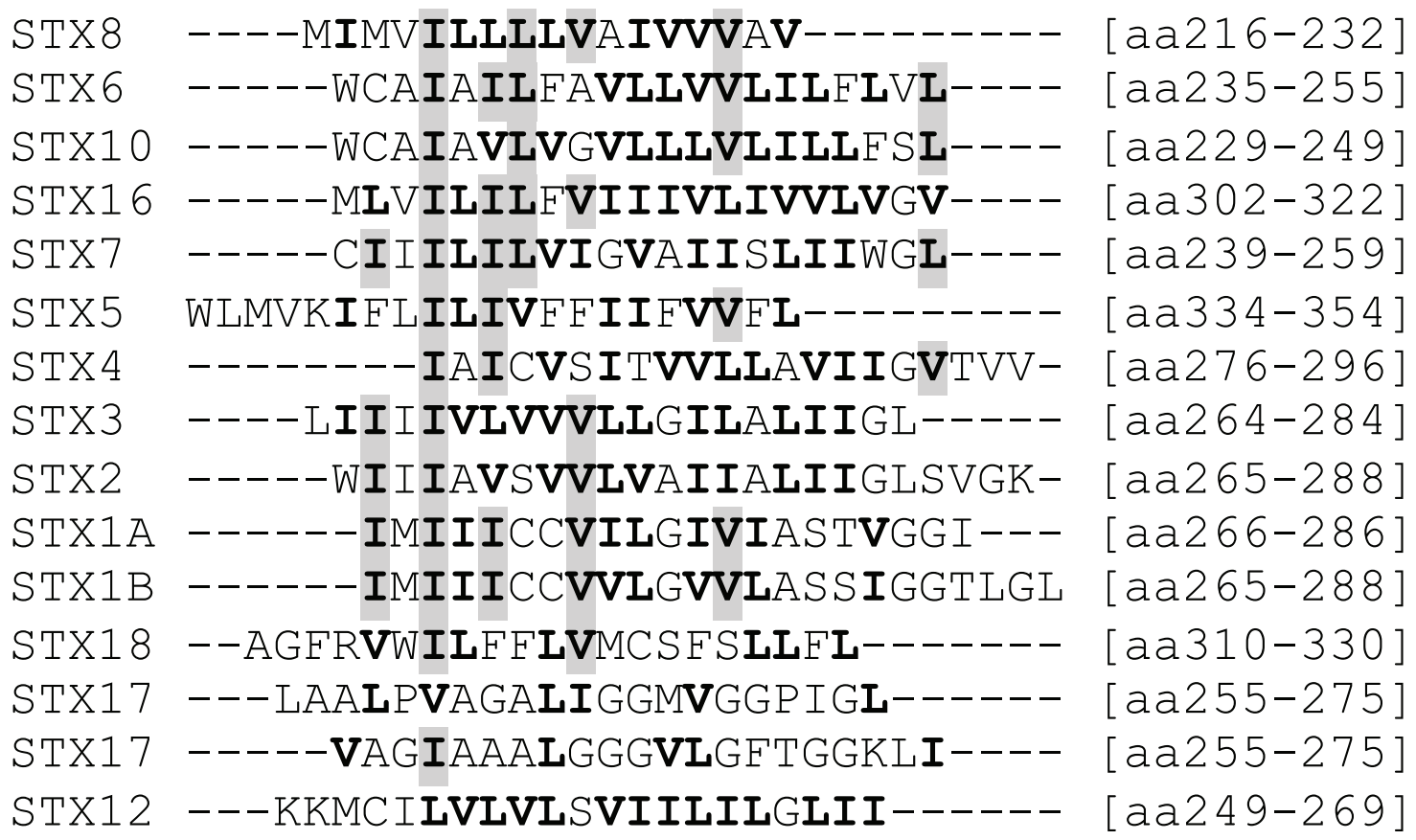


**Fig. S3. Alignment of transmembrane domain amino acid sequences of syntaxins.** CLUSTAL O alignment of transmembrane (TM) domain amino acid (aa) sequences of human syntaxins. Isoforms are indicated, followed by aa sequences and position of the TM in the respective full-length protein in brackets. Bolt lettering indicates Isoleucine (I), Leucine (L) and Valine (V) residues in similar positions. Conserved positions are highlighted in grey.